Research Article

Journal of RAMAN SPECTROSCOPY

Received: 21 October 2008 Accepted: 27 January 2009 Published online in Wiley Interscience: 16 March 2009

(www.interscience.wiley.com) DOI 10.1002/jrs.2255

Direct visual evidence for the chemical mechanism of surface-enhanced resonance Raman scattering via charge transfer: (II) Binding-site and quantum-size effects

Mengtao Sun,[a]* Shasha Liu,[b] Zhipeng Li,[a] Jianmin Duan,[b] Maodu Chen,[b] and Hongxing Xu[a,c]

We describe quantum-size and binding-site effects on the chemical and local field enhancement mechanisms of surface-enhanced resonance Raman scattering (SERRS), in which the pyridine molecule is adsorbed on one of the vertices of the Ag_{20} tetrahedron. We first investigated the influence of the binding site on normal Raman scattering (NRS) and excited state properties of optical absorption spectroscopy. Second, we investigated the quantum-size effect on the electromagnetic (EM) and chemical mechanism from 300 to 1000 nm with charge difference density. It is found that the strong absorption at around 350 nm is mainly the charge transfer (CT) excitation (CT between the molecule and the silver cluster) for large clusters, which is the direct evidence for the chemical enhancement mechanism for SERRS; for a small cluster the strong absorption around 350 nm is mainly intracluster excitation, which is the direct evidence for the EM enhancement mechanism. This conclusion is further confirmed with the general Mie theory. The plasmon peak in EM enhancement will be red-shifted with the increase of cluster size. The influence of the binding site and quantum-size effects on NRS, as well as chemical and EM enhancement mechanisms on SERRS, is significant.

Supporting information may be found in the online version of this article.

Keywords: chemical enhancement; charge transfer; SERRS; binding site; quantum size

Introduction

Surface-enhanced Raman scattering (SERS) is a powerful tool for obtaining chemical information of molecules on roughened metal substrates.[1–5] The enormous enhancement of the Raman signal results from electromagnetic (EM) and chemical mechanisms.[6–15] The EM enhancement is caused by the strong surface plasmon resonance of curved metal surfaces coupled to the incident light.[6–10] The chemical enhancement can be considered similarly to a resonance Raman process between the ground electronic state of the molecule–metal complex and its new excited levels arising from charge transfer (CT) between the metallic surface and the adsorbed molecule, which results in some Raman peaks being selectively enhanced enormously.[11–15]

With the visual method of charge difference density, we have observed the intracluster excitation and CT (between molecule and metal) excitation on resonant electronic transitions (Fig. 5 in Ref. [15]), which are the direct evidence for EM and chemical mechanism, respectively, on surface-enhanced resonance Raman scattering (SERRS).[10] The model in Ref. [15] assumes that pyridine adsorbed on the surface of the Ag_{20} tetrahedron (S-complex, Fig. 2) and the Ag_{20} cluster are part of large nanoparticles. Several theoretical studies have revealed that the absorption properties of a 20-atom silver tetrahedral cluster behave very similar to the plasmon excitation observed in nanoparticles, and the Raman enhancement due to the S-complex is comparable to that on large nanoparticles (>10 nm).[15–17]

As pointed out by Zhao *et al*.[16] the unique structure of the Ag_{20} tetrahedron allows us to study two very different binding sites. Apart from the S-complex, there is a V-complex model where the pyridine is adsorbed onto one of its vertices, which is an ad-atom site. By comparing the SERS spectra calculated with these S- and V-complex models, we can investigate the influence of different binding sites[16] on the SERS spectrum. By comparing the different excitation mechanisms on resonant electronic transitions at different binding sites with the same incident light, we can reveal the influence of the binding site on the enhancement mechanisms on SERRS. If the Ag_{20} cluster is considered as a part of large nanoparticles for the S-complex ($R \gg R_1$ in Fig.1(a)), and the size for V-complex remains as it is, we can study the influence of quantum size of the cluster on the SERS spectra as well as the enhancement mechanisms on SERRS.

* *Correspondence to: Mengtao Sun, Beijing National Laboratory for Condensed Matter Physics, Institute of Physics, Chinese Academy of Sciences, Beijing, 100190, P. R. China. E-mail: mtsun@aphy.iphy.ac.cn*

a *Beijing National Laboratory for Condensed Matter Physics, Institute of Physics, Chinese Academy of Sciences, Beijing, 100190, P. R. China*

b *School of Physics and Optoelectronic Technology, and Department of Chemistry, Dalian University of Technology, Dalian, 116024, P. R. China*

c *Division of Solid State Physics, Lund University, Lund 22100, Sweden*

Journal of RAMAN SPECTROSCOPY

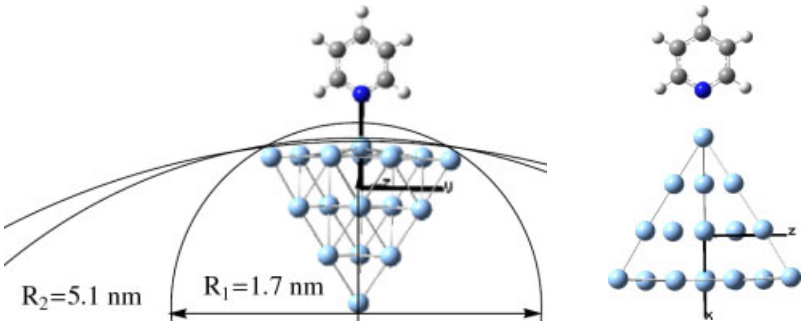

Figure 1. Configurations of (a) S-complex and (b) V-complex having C_S symmetry (taken from Ref. [15]. This figure is available in colour online at www.interscience.wiley.com/journal/jrs.

Experimentally, Peyser-Capadona *et al*.[18] have shown that a small (2–8 atoms) silver cluster encapsulated in a dendrimer or peptide scaffold can produce single-molecule Raman scattering characteristic of the scaffold. Theoretically, Jensen *et al*.[17] have studied the size dependence of the enhanced Raman scattering of pyridine adsorbed on Ag_n ($n = 2–8, 20$) clusters, and the results showed that both the absorption and Raman scattering properties depend strongly on the cluster size and adsorption site.

In this paper, we calculated the normal Raman scattering (NRS) spectrum, and describe the chemical and local field enhancement mechanisms of SERRS for the V-complex from 300 to 1000 nm with charge difference density. The NRS, absorption spectra and enhancement mechanisms for the V- and S-complex are directly compared. It is found that the binding site and the quantum size effects can significantly influence the profile of NRS spectrum as well as the enhancement mechanisms on SERRS at same incident wavelength.

Method

In quantum chemical calculations, tetrahedral Ag_{20} is used for the model of the nanoparticle, which is a relaxed fragment of the face-centered cubic (fcc) lattice of bulk silver and which is one of the local minima for the Ag_{20} cluster.[16] For this tetrahedral Ag_{20}, there are two very different binding sites (S- and V-complex, see Fig. 1). The former consists of an on-top binding to one of its four faces, which represents a (111) surface of fcc silver, while the latter consists of binding onto one of its vertices, which represents an ad-atom site.[16] In this paper, the ground-state geometries of the pyridine–Ag_{20} cluster for the V-complex was optimized with density functional theory (DFT)[19] using B3PW91 functional,[20] LANL2DZ basis set[21] for Ag, and 6-31G basis set for C, N and H. The SERS spectra of pyridine–Ag_{20} clusters were calculated with the same method at the zero frequency. It should be noted that the SERS spectrum calculated with Eqn (1) in Ref. [16] was obtained by averaging over all orientations of the cluster with respect to the electric field. The electronic structures of pyridine–Ag_{20} were calculated by the time-dependent density functional theory (TD-DFT) method[22] and the same functional and basis set. All above-mentioned quantum chemical calculations were performed with the Gaussian 03 suite.[23]

The Fermi energy levels of tetrahedral Ag_{20}, S-complex and V-complex, and the energy levels of highest occupied molecular orbital (HOMO) and lowest unoccupied molecular orbital (LUMO) of tetrahedral Ag_{20} were calculated with the DFT method, the local density approximation with the Perdew–Zunger parameterization (LDA-PZ) functional, the double zeta polarized (DZP) basis set, and 300 K for electron temperature, which were calculated with Virtual NanoLab.[24]

The charge difference density[25] was employed to visualize intracluster excitation and CT (between pyridine and Ag_{20} cluster) excitation, which are the direct visual evidence for the EM enhancement mechanism and chemical enhancement mechanism, respectively.

To study the influence of the binding-site effect on the EM enhancement mechanism, we calculated the EM enhancement of the silver tetrahedral nanoparticle (of side length 50 nm) at the incident light of 632.8 nm, using the finite difference time domain (FDTD) method.[26] To show the influence of the quantum-size effect on the EM enhancement mechanism, we calculated the EM enhancement for nanoparticles with different sizes in the range from 300 to 800 nm, using the generalized Mie theory.[27]

Discussion

Binding-site and quantum-size effect on NRS

Because of the coupling interaction between pyridine and the Ag_{20} clusters, the charge redistribution when forming the complexes between pyridine and Ag_{20} clusters (CT is 0.181 e and 0.166 e for the V-complex and the S-complex, respectively) results in a large static electronic polarizability (Table 1) and a static chemical enhancement to NRS (Fig. 2). Comparing the NRS of the V-complex with that of S-complex (Fig.2 in Ref. [15]), the intensity of ring stretch (1588 cm^{-1}) of the V-complex is much larger than that of the S-complex (1582 cm^{-1}), resulting from different chemical environments of the hydrogens close to the N atom, which is the binding-site effect. By comparing the calculated results and the experimental reports in Refs [16, 28], we find that the NRS spectrum of the S-complex is similar to the experimental reports.

Table 1. Calculated static electronic polarizability components in a.u. The Cartesian coordinate can be seen from Fig. 1

	xx	*yy*	*zz*
Pyridine	63.305	66.190	18.751
V-complex	1009.377	886.256	920.188
S-complex	1101.587	905.737	876.867

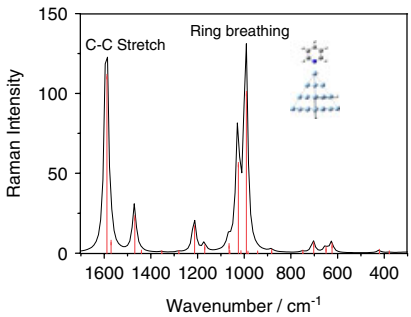

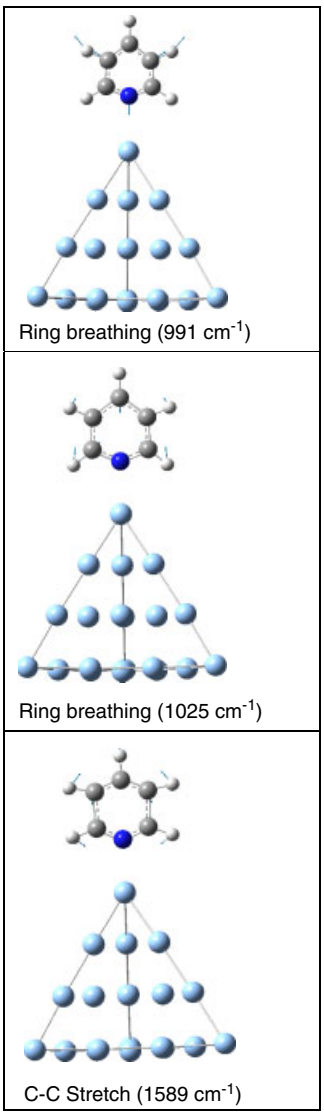

Figure 2. The simulated SERS (normal Raman scattering) spectrum of the V-complex. The scale factor of the wavenumbers is set at 0.96 in our calculations. This figure is available in colour online at www.interscience.wiley.com/journal/jrs.

This is easy to understand since the nanoparticle is large in the experiments and the S-complex is used to simulate the NRS for large nonoparticle. By comparing the enhanced intensity of SERRS, in general, the intensity of the SERS spectrum for the V-complex is larger than that for the S-complex. It can be interpreted by the binding site (hot site) effect of the EM mechanism. From Fig. 3,

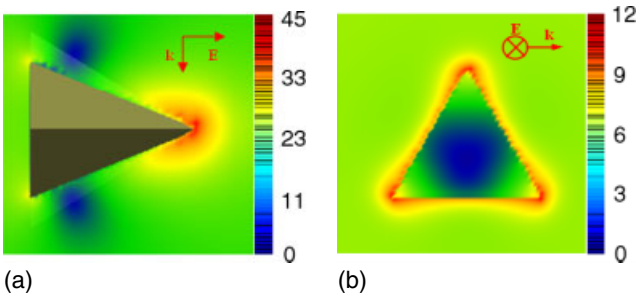

Figure 3. The electromagnetic enhancements ($|E|$) of silver tetrahedral nanoparticles (side length 50 nm) at incident lights of 632.8 nm. (a) and (b) are for the case of a cut along the threefold axis of the tetrahedron and for the case shown the field at the triangular surface, respectively. The color bars of $|E|$ are shown at the right of the pictures. The enhancements of SERS intensities, approximated as the second power of the field enhancement factor $|E|$, are $|E|$. This figure is available in colour online at www.interscience.wiley.com/journal/jrs.

the EM enhancement at the vertices is obviously larger than that at the surface. The calculated NRS of the V-complex (binding site effect) needs similar experimental confirmation in such small tetrahedrons in future.

Optical absorption spectra and enhanced mechanism of SERRS

The calculated optical absorption spectra for the V-complex and the S-complex can be seen from Fig. 4(a) and (b). It is found that there is little influence on the local binding site to the profile of the absorption spectra in the molecule–metal complex, but there is more CT for the S-complex than for the V-complex. The qualitative reason is that the EM enhancement at the vertices is obviously larger than that on the surface, which can be seen from Fig. 3.

With the visual method of the charge difference density, we investigated the intracluster excitation and the CT excitation on the resonant electronic transition (Supporting Information). It is found that the enhanced mechanism on SERRS at the strongest absorption around 350 nm is significantly different. For the S-complex, the SERRS spectra is contributed by the chemical mechanism via CT at the strongest absorption (~350 nm),[15] while the SERRS spectra are contributed by the EM mechanism via intracluster excitation at the strongest absorption (~350 nm) for the V-complex. It can be interpreted by the optical properties of the isolated tetrahedral Ag_{20}. We calculated the optical absorption of the isolated tetrahedral Ag_{20} with TD-DFT/B3PW91/LANL2DZ//DFT/B3PW91/LANL2DZ, which can be seen from Fig. 4(c). It is found that the strongest optical absorption is around 350 nm for the isolated tetrahedral Ag_{20}. The EM enhancement at the vertices for the V-complex is obviously larger than at the surface for the S-complex at around 350 nm, which can be seen from Fig. 3. So, different binding sites can strongly influence the enhancement mechanisms for SERRS at the same incident wavelength. The enhancement mechanism of the V-complex at ~350 nm is similar to our previous results on the pyridine–Ag_2 complex,[29] because they are all based on the model of the ad-atom site. Since the S-complex and the V-complex are used to simulate the SERS for naniparticles of large and small sizes, respectively, the quantum size of the nanoparticle is expected to influence the enhancement mechanism on SERRS.

Using the generalized Mie theory[27] we calculated the EM enhancement at the point A, which is 1 nm above the surface of the silver nanoparticle (Fig. 5). The direction of the wave

Journal of RAMAN SPECTROSCOPY

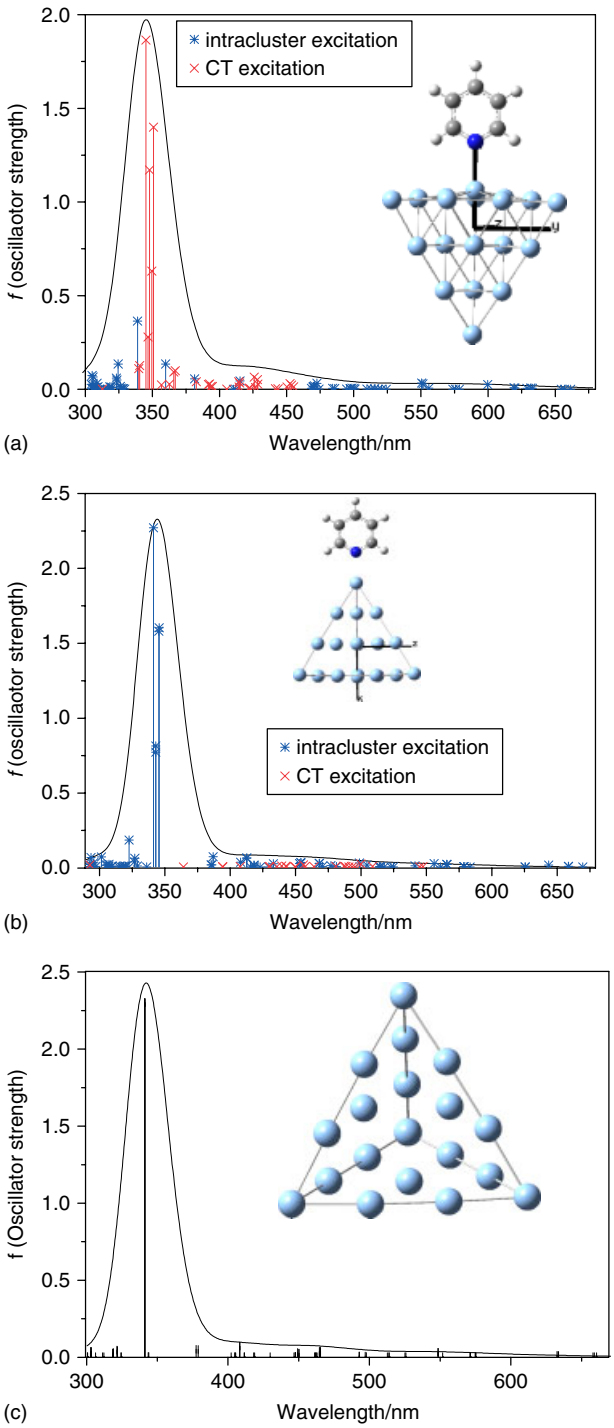

Figure 4. (a) The optical electronic state absorption of the S-Complex from Ref. [15], (b) for V-complex and (c) for isolated Ag_{20} tetrahedron. The intracluster and CT on resonant electronic transitions at lowest 100 singlet excited states have been shown. This figure is available in colour online at www.interscience.wiley.com/journal/jrs.

vector and polarization is shown in the inset. The multipole order n is here truncated at $N = 12$, which is enough for the convergence. We considered two types of radius: 20 and 50 nm. For $R = 50$ nm, the local enhancement factor for the intensity is about 31 in the wavelength range 400 to ~700 nm, which means that the EM enhancement gives the main contribution to the SERS

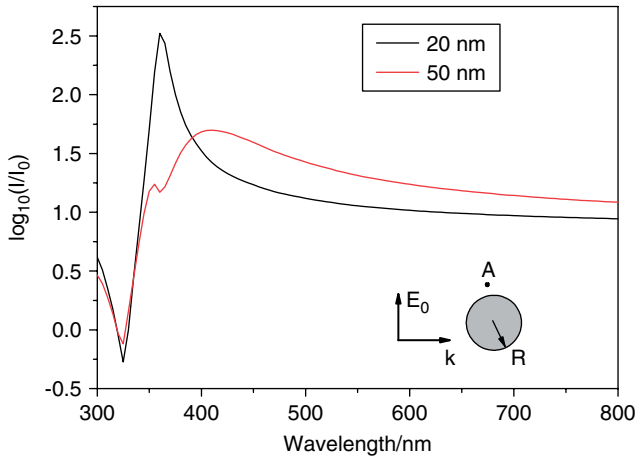

Figure 5. The EM intensity enhancement ($I = |E|^2$) at point A as a function of the incident wavelength. A is 1 nm away from the upper surface of the Ag nanoparticle ($R = 20$, 50 nm). Inset shows the direction of the wave vector and the polarization. This figure is available in colour online at www.interscience.wiley.com/journal/jrs.

enhancement in this range. For $R = 20$ nm, the enhancement is significant around 360 nm, while for $\lambda > 400$ nm, it is lower than the case of $R = 50$ nm.

By comparing Fig. 6 (a)and (b), one can find that the lowest CT excited state for the S-complex is 450 nm, while the lowest CT excited state for the V-complex is 550 nm. We interpret this with orbital energy level and their Fermi levels. The CT from the metal to pyridine on resonant electronic transition is from the Fermi level of the S-complex and that of the V-complex to the LUMO of pyridine, respectively, for the lowest CT excited state (Fig. 7(a)). From Fig. 7(b), the Fermi level of the V-complex is slightly higher than that of the S-complex, and $E_{\text{Fermi}}(\text{V} - \text{complex}) - E_{\text{Fermi}}(\text{S} - \text{complex}) = 0.083$ eV, so the CT excited states for V-complex are red-shifted compared to those of the S-complex.

For the V-complex, all of them are the intracluster CT excited states on the electronic collective oscillation excitation at ~350 nm, so SERRS at ~350 nm for the V-complex is contributed by local field enhancement effect by plasmon collective oscillations. Our previous theoretical study on SERRS of the pyridine–Ag_2 complex is a simplified model of the V-complex, and the SERRS at ~379 nm with strong oscillator strength is also contributed by the local field effect by plasmon collective oscillations. The red shift of the strong absorption peak (~30 nm) is from the size effect of the cluster.

So, the enhanced mechanism for the V-complex is clear now, according to the charge difference densities in the range of 670–300 nm in Supporting Information. When the energy of the incident laser light is below 670 nm, the Raman spectra is SERS, not SERRS, and the mechanism of SERS is static chemical enhancement. When the incident laser light is between 670 and 550 nm, the excited states are the intracluster excitation, so the SERS is contributed by EM enhancement. When the incident laser wavelength is between 550 and 365 nm, the excitations are a mixture of intracluster and CT excited states, and therefore the SERRS is contributed by the mixture of chemical and EM enhancements via CT from Ag_{20} cluster to pyridine. When the incident light is below 365 nm, SERRS is contributed by the local field enhancement on intraluster collective oscillation excitation, except for S_{98}.

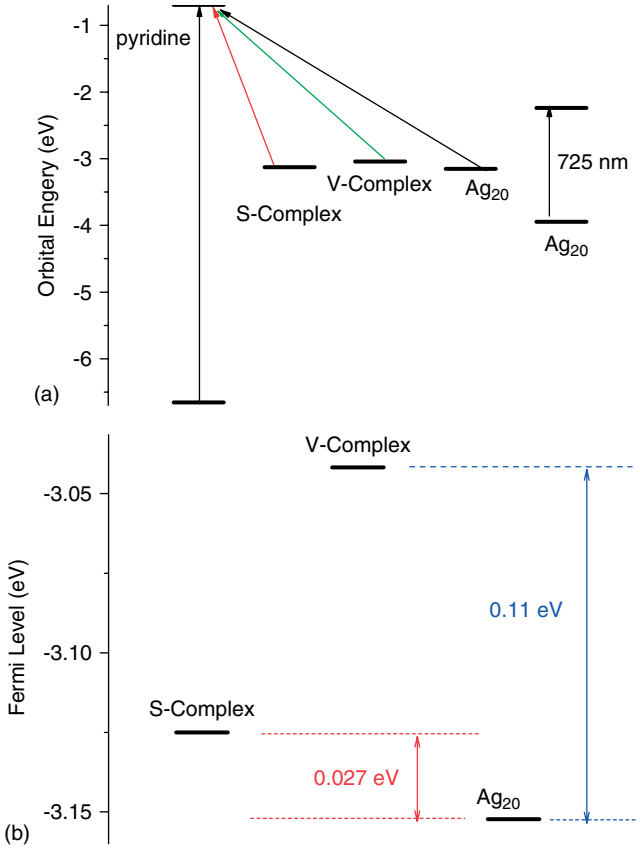

Figure 6. (a) The molecular orbital energy levels of HOMO and LUMO of the S-complex and V-complex, and (b) the Fermi energy levels of Ag_{20} cluster, S-complex and V-complex. This figure is available in colour online at www.interscience.wiley.com/journal/jrs.

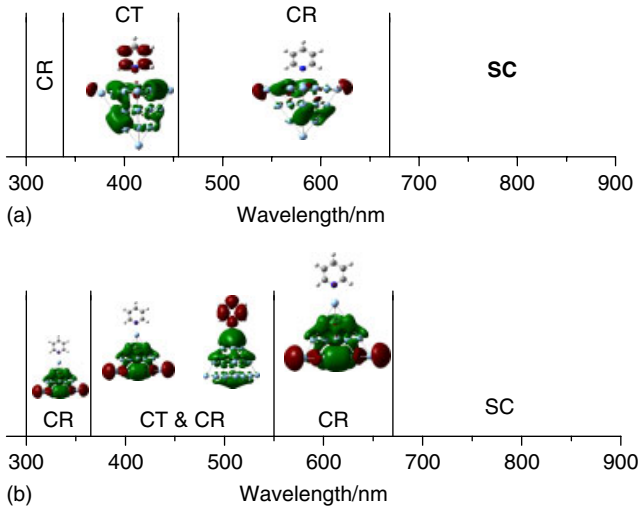

Figure 7. The chemical and electromagnetic field enhancement mechanisms at different regions of frequencies for (a) S-complex from Ref. [15] and (b) for V-complex. The abbreviations SC, CR and CT stand for static chemical enhancement, charge redistribution on intracluster excitation and charge transfer between the molecule and the metal cluster. The two inserts are the charge difference densities for the intracluster excitation and CT excitation (charge transfer from Ag_{20} cluster to pyridine), respectively, where the green and the red stand for hole and electron, respectively. This figure is available in colour online at www.interscience.wiley.com/journal/jrs.

Conclusions

The NRS spectrum, absorption spectrum and enhancement mechanism (via intracluster or CT excitations) have been compared between the V-complex and the S-complex. It is found that there is no influence on the absorption spectra when the molecule is adsorbed on different sites. The NRS spectrum and enhancement mechanism are strongly influenced by different binding-site and quantum-size effects for the V-complex and the S-complex.

Acknowledgements

This work was supported by the National Natural Science Foundation of China (Grant Nos. 10874234, 20703064, 10874233, 10625418 and 10604012), the Sino–Swedish Collaborations on Nanophotonics and Nanoelectronics (2006DFB02020), the National Basic Research Project of China (Grant Nos. 2009CB930701, 2007CB936804) and the 'Bairen' projects of CAS.

Supporting information

Supporting information may be found in the online version of this article.

References

[1] M. Fleischman, P. J. Hendra, A. J. McQuillan, *Chem. Phys. Lett.* **1974**, *26*, 123.
[2] D. L. Jeanmaire, R. P. V. Duyne, *J. Electroanal. Chem.* **1977**, *84*, 1.
[3] M. G. Albrecht, J. A. Creighton, *J. Am. Chem. Soc.* **1977**, *99*, 5215.
[4] M. Moskovits, *Rev. Mod. Phys.* **1985**, *57*, 783.
[5] A. Otto, I. Mrozek, H. Grabhorn, W. Akemann, *J. Phys. Condens. Matter.* **1992**, *4*, 1143.
[6] K. Kneipp, Y. Wang, H. Kneipp, L. T. Perelman, I. Itzkan, R. R. Dasari, M. S. Feld, *Phys. Rev. Lett.* **1997**, *78*, 1667.
[7] H. Xu, E. J. Bjerneld, M. Käll, L. Borjesson, *Phys. Rev. Lett.* **1999**, *83*, 4357.
[8] M. Moskovits, *J. Raman Spectrosc.* **2005**, *36*, 485.
[9.] K. Kneipp, H. Kneipp, M. Moskovits (eds), in *Surface-enhanced Raman Scattering, Physics and Applications*, Springer: Heidelberg, **2006**.
[10] R. L. Garrell, *Anal. Chem.* **1989**, *61*, 401A.
[11] E. J. Liang, W. Kiefer, *J. Raman Spectrosc.* **1996**, *12*, 879.
[12] A. Otto, *J. Raman Spectrosc.* **2005**, *36*, 497.
[13] J. F. Arenas, I. López-Tocón, J. L. Castro, S. P. Centeno, M. R. López-Ramírez, J. C. Otero, *J. Raman Spectrosc.* **2005**, *36*, 515.
[14] J. R. Lombardi, R. L. Birke, *J. Phys. Chem. C* **2008**, *112*, 5605.
[15] M. T. Sun, S. S. Liu, M. D. Chen, H. X. Xu, *J. Raman Spectrosc.* **2009**, *40*, 137.
[16] L. L. Zhao, L. Jensen, G. C. Schatz, *J. Am. Chem. Soc.* **2006**, *128*, 2911.
[17] L. Jensen, L. L. Zhao, G. C. Schatz, *J. Phys. Chem. C* **2007**, *111*, 4756.
[18] L. Peyser-Capadona, J. Zheng, J. L. Gonzalez, T. H. Lee, S. A. Patel, R. M. Dickson, *Phys. Rev. Lett.* **2005**, *94*, 058301.
[19] P. Hohenberg, W. Kohn, *Phys. Rev.* **1964**, *136*, B864.
[20] (a) A. D. Becke, *Phys. Rev. A* **1988**, *38*, 3098; (b) J. P. Perdew, J. A. Chevary, S. H. Vosko, K. A. Jackson, M. R. Pederson, D. J. Singh, C. Fiolhais, *Phys. Rev. B* **1992**, *46*, 6671.
[21] P. J. Hay, W. R. Wadt, *J. Chem. Phys.* **1985**, *82*, 270.
[22] E. K. U. Gross, W. Kohn, *Phys. Rev. Lett.* **1985**, *55*, 2850.
[23] M. J. Frisch, G. W. Trucks, H. B. Schlegel, G. E. Scuseria, M. A. Robb, J. R. Cheeseman, J. A. Montgomery, T. Vreven Jr, K. N. Kudin, J. C. Burant, J. M. Millam, S. S. Iyengar, J. Tomasi, V. Barone, B. Mennucci, M. Cossi, G. Scalmani, N. Rega, G. A. Petersson, H. Nakatsuji, M. Hada, M. Ehara, K. Toyota, R. Fukuda, J. Hasegawa, M. Ishida, T. Nakajima, Y. Honda, O. Kitao, H. Nakai, M. Klene, X. Li, J. E. Knox, H. P. Hratchian, J. B. Cross, C. Adamo, J. Jaramillo, R. Gomperts, R. E. Stratmann, O. Yazyev, A. J. Austin, R. Cammi, C. Pomelli, J. W. Ochterski, P. Y. Ayala, K. Morokuma, G. A. Voth, P. Salvador, J. J. Dannenberg, V. G. Zakrzewski, S. Dapprich,

A. D. Daniels, M. C. Strain, O. Farkas, D. K. Malick, A. D. Rabuck, K. Raghavachari, J. B. Foresman, J. V. Ortiz, Q. Cui, A. G. Baboul, S. Clifford, J. Cioslowski, B. B. Stefanov, G. Liu, A. Liashenko, P. Piskorz, I. Komaromi, R. L. Martin, D. J. Fox, T. Keith, M. A. Al-Laham, C. Y. Peng, A. Nanayakkara, M. Challacombe, P. M. W. Gill, B. Johnson, W. Chen, M. W. Wong, C. Gonzalez, J. A. Pople, *Gaussian 03, Revision E. 01*, Gaussian: Wallingford, **2004**.

[24] M. Brandbyge, J.-L. Mozos, P. Ordejon, J. Taylor, K. Stokbro, *Phys. Rev. B* **2002**, *65*, 165401.

[25] M. T. Sun, *J. Chem. Phys.* **2006**, *124*, 054903.

[26] K. S. Kunz, R. J. Luebber, *The Finite Difference Time Domain Method for Electromagnetics*, CRC Press: LLC, Boca Raton, FL, **1993**.

[27] H. X. Xu, *J. Opt. Soc. Am. A* **2004**, *21*, 804.

[28] J. T. Golab, J. R. Sprague, K. T. Carron, G. C. Schatz, R. P. Van Duyne, *J. Chem. Phys.* **1988**, *88*, 7942.

[29] M. T. Sun, S. B. Wan, Y. J. Liu, J. Yu, H. X. Xu, *J. Raman Spectrosc.* **2008**, *39*, 402.

